



HAL
open science

Monitoring of artificial water reservoirs in the Southern Brazilian Amazon with remote sensing data

Damien Arvor, Felipe Daher, Thomas Corpetti, Marianne Laslier, Vincent Dubreuil

► **To cite this version:**

Damien Arvor, Felipe Daher, Thomas Corpetti, Marianne Laslier, Vincent Dubreuil. Monitoring of artificial water reservoirs in the Southern Brazilian Amazon with remote sensing data. SPIE 2016, Sep 2016, Edimbourg, United Kingdom. 10.1117/12.2241905 . halshs-01518623

HAL Id: halshs-01518623

<https://shs.hal.science/halshs-01518623>

Submitted on 18 Apr 2020

HAL is a multi-disciplinary open access archive for the deposit and dissemination of scientific research documents, whether they are published or not. The documents may come from teaching and research institutions in France or abroad, or from public or private research centers.

L'archive ouverte pluridisciplinaire **HAL**, est destinée au dépôt et à la diffusion de documents scientifiques de niveau recherche, publiés ou non, émanant des établissements d'enseignement et de recherche français ou étrangers, des laboratoires publics ou privés.

Monitoring of artificial water reservoirs in the Southern Brazilian Amazon with remote sensing data

Damien Arvor^a, Felipe Daher^a, Thomas Corpetti^a, Marianne Laslier^a, and Vincent Dubreuil^a

^aUMR 6554 CNRS, LETG-Rennes-COSTEL, Université Rennes 2, Place du Recteur Henri Le Moal, Rennes, France

ABSTRACT

The agricultural expansion in the Southern Brazilian Amazon has long been pointed out due to its severe impacts on tropical forests. But the last decade has been marked by a rapid agricultural transition which enabled to reduce pressure on forests through (i) the adoption of intensive agricultural practices and (ii) the diversification of activities. However, we suggest that this new agricultural model implies new pressures on environment and especially on water resources since many artificial water reservoirs have been built to ensure crop irrigation, generate energy, farm fishes, enable access to water for cattle or just for leisure. In this paper, we implemented a method to automatically map artificial water reservoirs based on time series of Landsat images. The method was tested in the county of Sorriso (State of Mato Grosso, Brazil) where we identified 521 water reservoirs by visual inspection on very high resolution images. 68 Landsat-8 images covering 4 scenes in 2015 were pre-classified and a final class (Terrestrial or Aquatic) was determined for each pixel based on a Dempster-Shafer fusion approach. Results confirmed the potential of the methodology to automatically and efficiently detect water reservoirs in the study area (overall accuracy = 0.952 and Kappa index = 0.904) although the methodology underestimates the total area in water bodies because of the spatial resolution of Landsat images. In the case of Sorriso, we mapped 19.4 km² of the 20.8 km² of water reservoirs initially delimited by visual interpretation, i.e. we underestimated the area by 5.9%.

Keywords: Mato Grosso, Water bodies, Landsat, Time series, data fusion

1. INTRODUCTION

The agricultural expansion in the Southern Brazilian Amazon has long been pointed out as a threat to the environment.¹ The rapid conversion of native vegetation to croplands has dramatically impacted the Brazilian cerrados and tropical forests.² This is especially true in the Brazilian state of Mato Grosso where the total cultivated area in soybean, maize and cotton (over 8.6 millions hectares³) has long been associated with high deforestation rates.⁴

However, the last decade has been marked by a rapid agricultural transition based on (i) the adoption of intensive agricultural practices such as double-cropping systems including soy-cotton and soy-maize crops,⁵ (ii) the diversification of activities including pig, poultry and fish farming, and (iii) the development of irrigation systems, mainly to prevent harvest losses for the second crop. This transition enabled to efficiently reduce pressure on forests and savannas as proven by the dramatic decline in deforestation rates observed since 2005.^{6,7}

Nonetheless, while reducing pressure on native vegetation, we suggest that this new agricultural model may imply new pressures on environment and especially on water resources. Indeed, many artificial water reservoirs have been built to ensure crop irrigation, generate energy, enable access to water for cattle and overall to farm fishes. In 2015, the Ministry of Fisheries and Aquiculture (*Ministério da Pesca e Aquicultura*, MPA) launched the *Safra da Pesca e Aquicultura* (PSPA) program with the objective to support the sustainable development of fishing and aquiculture activities. In this program, R\$2 billion of incentives are available through credit lines for small, medium and large producers to improve the production and productivity of fishing activities [12]. As a consequence, the number of water reservoirs is expected to increase in the next future.

Further author information: (Send correspondence to D.A.)

D.A.: E-mail: damien.arvor@univ-rennes2.fr, Telephone: +33 (0)2 99 14 18 68

In this regard, the Decree n. 4895 (11/2003) regulates the use of water resources for aquiculture at national level. In Mato Grosso, the Law n. 9.619 (10/2011), updated in 2013 (Law n.9.933/2013), defines the pisciculture activity and especially states that : *"fish farmers with up to 5 hectares of water tank or up to 10.000 m³ are exempted from environmental licensing as well as from the payment of registration fees."* Monitoring the emergence of water reservoirs in the Amazon thus appears to be essential to better understand the last step of land use changes that characterizes the agricultural transition in the Southern Amazon.

In this paper, we intend to test the suitability of Landsat time series to automatically map artificial water reservoirs in the county of Sorriso (State of Mato Grosso, Brazil), known as the national leader for soybean production.

2. STUDY AREA

The study area is located in the Southern Amazon Brazilian State of Mato Grosso, which has long been studied due to the dramatic land use changes that occurred there since the 1970s. Indeed, the occupation of Mato Grosso was supported by the federal government to benefit from the natural resources (especially favorable climate conditions^{8,9}) in order to develop an extensive commodity-oriented agriculture.¹⁰ In this regard, the municipality of Sorriso serves as a best example. Sorriso was created in 1986 and covers an area of 9.329 km² located along the BR-163 Cuiabá - Santarém transamazonian road. Sorriso is known as the main soybean producer at national scale with a cultivated area of 620.000 hectares, i.e. 65% of the total municipal area and yields higher than the national average (Table 1).

The agricultural expansion in Mato Grosso and especially in Sorriso has led to dramatic environmental impacts (i.e. deforestation). It also increased the economic vulnerability at local scale since 90% of the local economy is related to soybean production.¹¹ In order to limit the dependence on monoculture, many producers have decided to diversify the production, mainly with maize and cotton.^{5,12} For a few years, fish farming is also considered with special attention due to easy access to credits.¹³ In this regard, Sorriso appears as a leader at national level with a total fish production of 21.000 tons, i.e. 4.4% of the national production.

Table 1. Planted area, production and yield for soybean in 2014³

Name	Planted area (ha)	Production (Tons)	Yield (Kh/ha)
Brazil	30.308.231	86.760.520	2.866
Mato Grosso	8.628.608	26.495.884	3.076
Sorriso	635.000	1.981.800	3.146

3. DATA AND METHODS

3.1 Data

The county of Sorriso is covered by four Landsat scenes, i.e. Path/Row = 226/068, 226/069, 227/068, 227/069. For these scenes, we acquired 68 Landsat-8 images for the year 2015 (Table 2) through the USGS ESPA Ordering Interface (<http://espa.cr.usgs.gov> website). All images were geometrically corrected (L1T images) and with less than 50% cloud cover. Additionally, the cloud-shadow Fmask product¹⁴ was also ordered.

Table 2. Summary of Landsat images used for the classification

Scenes	226/068	226/069	227/068	227/069
Number of images	18	16	18	16

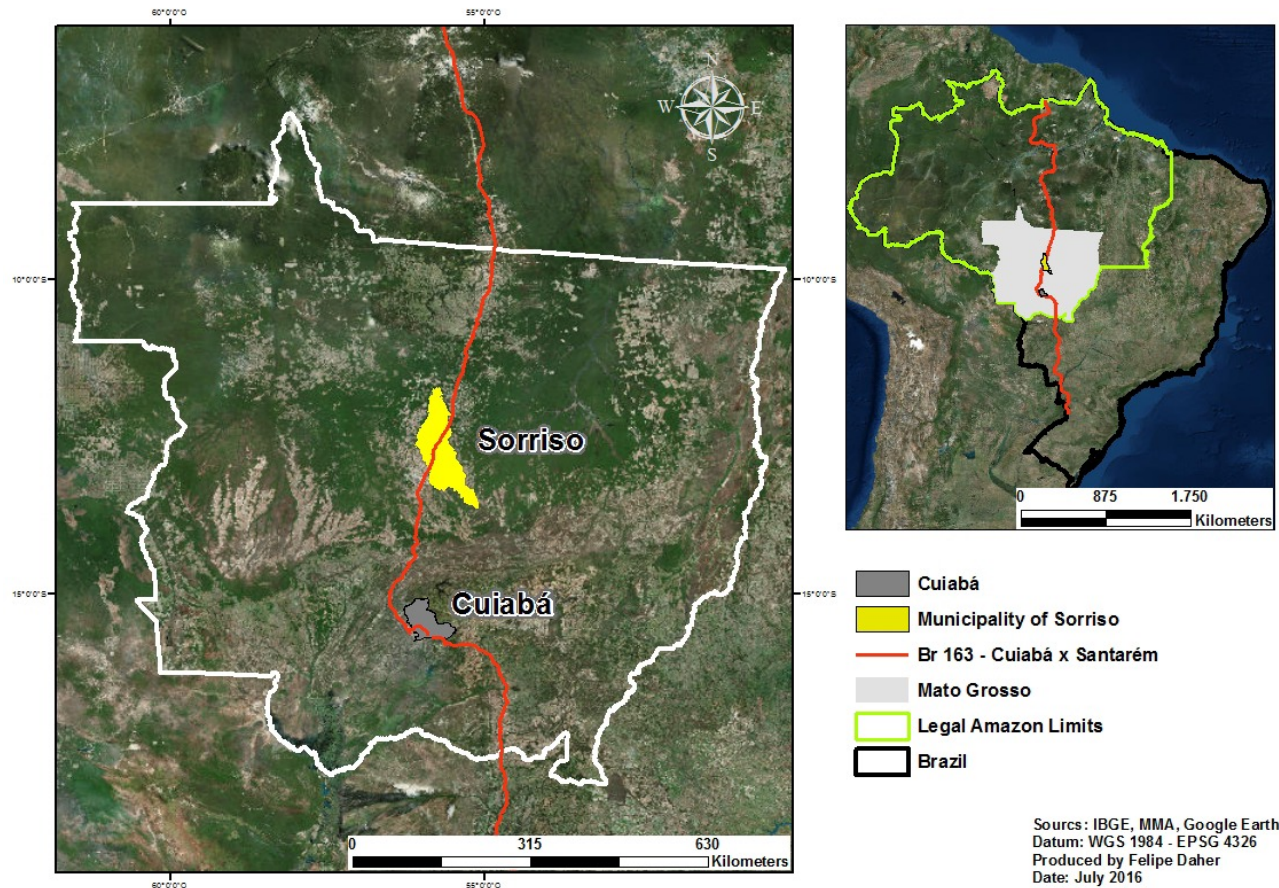


Figure 1. Location of the municipality of Sorriso, in the Sate of Mato Grosso (MT)

3.2 Pre-processing

All images were automatically calibrated in Top-of-Atmosphere reflectance and then pre-classified based on a method entirely described in Baraldi et al. (2006).¹⁵ This method was initially designed for Landsat TM and ETM+ images but its application to Landsat-8 is possible thanks to the continuity between Landsat satellites.¹⁶ The method assigns pixels to semantic spectral categories exclusively based on spectral rules. These spectral categories (up to 46 categories are discriminated) do not correspond to land cover classes but should rather be considered as semantic descriptions of spectral signatures.

3.3 Data fusion

For each scene, we organized time series of N pre-classifications. Each pixel is thus described by N observations, each of them referring to a spectral category. We thus intend to exploit this temporal information to derive a single land cover class associated with each pixel. Here, the land cover classes of interest are Terrestrial and Aquatic as proposed in the Land Cover Classification System (LCCS).¹⁷

To fuse the information into a single class, we rely on the Dempster-Shafer fusion approach.¹⁸ This approach belongs to the family of evidence theory where each class is represented with a belief function associated with uncertainties. The final decision is taken on the basis of mass functions using the Dempster's fusion rule in order to assign a single class to each pixel. In a remote sensing context, the Dempster-Shafer theory has mainly been applied to facilitate the decision process for the classification in many various applications (see¹⁹⁻²¹ for example).

Applying a Dempster-Shafer fusion approach first implies to set coefficient masses to be affected to each spectral category, i.e. define the probability for a pixel observed in a given spectral category to represent a

Terrestrial or Aquatic land cover class. In Baraldi et al. (2006),¹⁵ the spectral categories are not explicit in terms of land cover but potential corresponding land cover classes are proposed so that it is possible to set the coefficients masses by expertise.

Here we considered that only the spectral categories named "Deep Water or Shadow Spectral Categories" (DPWASH), "Shallow Water or Shadow Spectral Categories" (SLWAS) and "Turbid Water" (TWA) refer to water bodies. According to the authors, these three classes may be confused with shadow areas but since shadows are supposed to be already mapped by the Fmask product, we considered that they actually represent water pixels. We thus assigned a 100% probability to belong to the Aquatic land cover class for these three categories, i.e a mass of 1 (Table 3). For all other spectral categories, the masses are set to 0 so that any decision can be taken based on this information. We considered that, although a pixel is never classified as DPWASH, SLWASH or TWA, it does not mean that it might not correspond to an Aquatic land cover at any other period of the year. It is worth mentioning that this approach may not be fully justified in the present study since many images are available for the entire study year but it would be more relevant for areas where few images are available annually.

By setting the coefficient masses based on expertise, we did not set any uncertainty value, which is actually a major interest of the Dempster-Shafer fusion approach. Actually, the uncertainty was computed based on the rate of unobserved pixels in the image, i.e. the amount of cloud and shadow pixels as defined by the Fmask.¹⁴ With this approach, the objective was to give more importance to pixels classified in cloud-free images than to pixels observed in cloudy images. Concretely, the rate of unobserved pixels in the image was assigned to the uncertainty value. The coefficient masses for Aquatic and Terrestrial land cover classes were thus distributed proportionally to the expert-based coefficient masses. For example, a pixel classified as DPWASH in a image with a 40% rate of unobserved pixels was assigned the following coefficients masses: 0.4 for Uncertainty, 0.6 for Aquatic and 0 for Terrestrial land cover class.

All pre-classifications of the time series were finally merged together through the Dempster-Shafer fusion approach in order to get the final probability for a given pixel to belong to the Aquatic or Terrestrial land cover class.

3.4 Final classification

The fusion process produces four images (corresponding to the four scenes covering the study area) representing the pignistic probability for a pixel to belong to the Aquatic land cover class. The probability values range from 0.5 to 1. 0.5 is the minimum value indicating that any decision on the land cover class can be taken based on the available information.

These four images were then mosaicked by keeping only the probability value of pixels with the highest number of observations in overlaying areas covered by adjacent scenes.

All pixels with a pignistic probability higher than 0.5 were classified as Aquatic pixels (Class 2). Other pixels (probability = 0.5) were classified as Terrestrial. Pixels that are never observed are classified as 0 (No pixel of the present study fell in this category). Finally, the water areas were dilated by a one pixel size structuring element in order to better capture the water borders which are often covered by trees.

Table 3. Coefficient masses assigned to spectral categories according to their probability to correspond to Aquatic or Terrestrial land cover class

	Aquatic	Terrestrial	Uncertainty
Deep Water or Shadow	1	0	0
Shallow Water or Shadow	1	0	0
Turbid Water	1	0	0
All other spectral categories	0	0	0

3.5 Validation

The validation of the classification is based on a reference dataset where all artificial water bodies in Sorriso were visually mapped on Google Earth (fig. 2). Two types of water bodies were considered: 1) run-of-the-river dams, whose uses are various (irrigation, energy, fish farming, etc) and 2) excavated dams, usually designed to fish farming. In Sorriso, 571 artificial water reservoirs were thus manually mapped, i.e. 345 run-of-the-river dams and 226 excavated dams, for a total area of 20.77 km² of artificial water bodies.

Based on this reference dataset, the validation process consisted in defining a 500 m buffer around each water reservoir to get samples of Terrestrial land cover class. We then randomly selected 500 points of Aquatic (in the mapped water reservoirs) and 500 points of Terrestrial class (in the buffer areas). The classification was then validated based on these 1000 sample points by computing a confusion matrix and the associated statistics, i.e. Overall Accuracy and Kappa index.²²

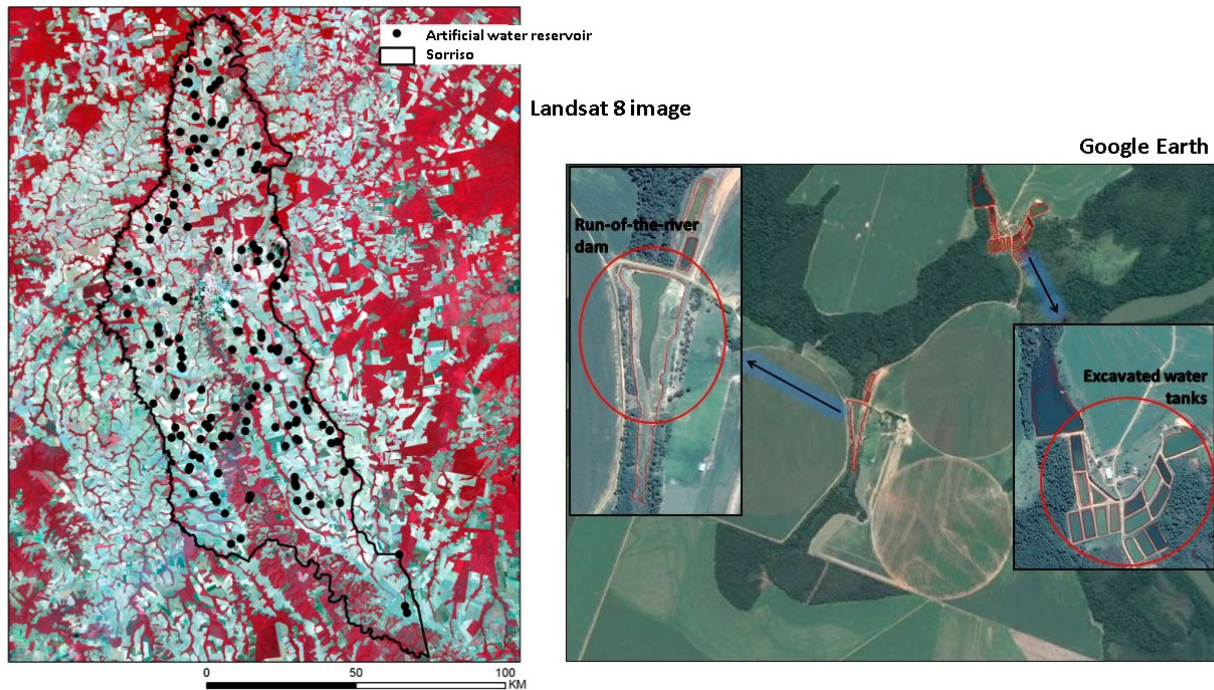


Figure 2. Map of water reservoirs visually detected in Sorriso based on Google Earth.

4. RESULTS

Results of the classification (fig. 4) illustrate the potential of the methodology to automatically and efficiently detect water reservoirs in the study area. This is statistically confirmed by the analysis of the confusion matrix (Table 4) characterized by high values for overall accuracy (O.A. = 0.952) and Kappa index (K = 0.904). On the one hand, few commission errors are detected, i.e. few Terrestrial pixels were classified as Aquatic. This may occur in three cases: 1) water reservoirs may have been manually delimited during the dry season so that the limits may not correspond exactly to what can be observed on a time series of remote sensing images, 2) pixels in natural water bodies (i.e. rivers) may have been selected as validation samples for the Terrestrial class and 3) cloud-shadows were not detected by Fmask and pre-classified as TWA, DPWASH or SLWASH spectral categories. On the other hand, the main confusion concerns omission errors, i.e. few pixels of Aquatic class were not detected on remote sensing images. This is especially true for small water bodies not observable at the Landsat spatial resolution. 43% of visually mapped reservoirs were smaller than 4 Landsat pixels and thus represented by mixed pixels. As a consequence, although the smallest reservoir classified was 396 m² large, only

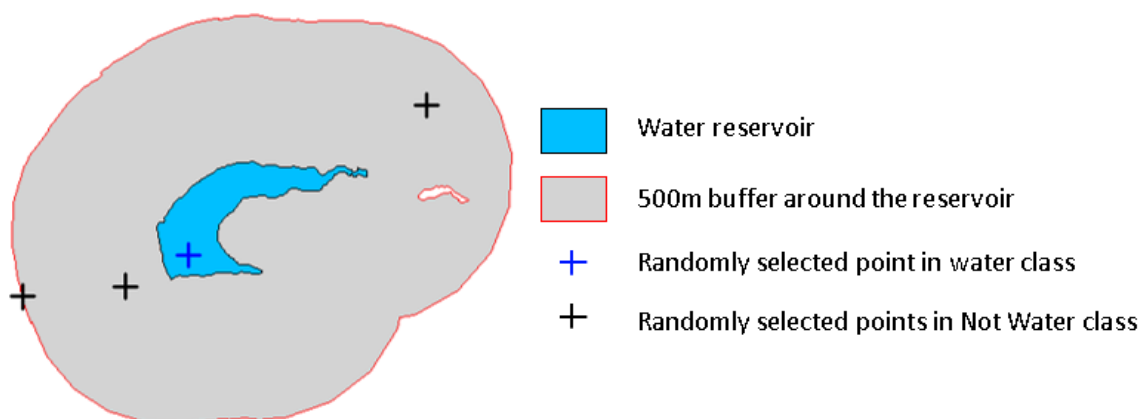


Figure 3. Example of randomly selected points for validation in both Aquatic and Terrestrial land cover classes.

79.3% of all water bodies mapped visually on high resolution images were detected on Landsat images, i.e. at least one pixel of the water reservoir has been classified as Aquatic. This level increases to 90% if we only consider water bodies larger than 1200 m².

Because of the spatial resolution of Landsat images, the methodology thus underestimates the area in water bodies. In the case of Sorriso, the methodology enabled to map 19.54 km² of the 20.8 km² of water reservoirs initially mapped by visual interpretation, i.e. the method underestimated the area by 5.9%.

Table 4. Confusion matrix for the 2015 classification.

		Classification		Producer's Accuracy
		Terrestrial	Aquatic	
Reference Data	Terrestrial	485	21	0.958
	Aquatic	27	473	0.946
User's Accuracy		0.947	0.957	
Overall Accuracy	0.952			
Kappa	0.904			

5. DISCUSSION

The method presented in this paper has proven to be efficient to automatically map water bodies. However, it is still limited to detect small water reservoirs because of the spatial resolution of Landsat data. It thus would be relevant to test a similar approach with higher spatial and temporal resolution data such as Sentinel-2. Such data may also be able to discriminate different types of water bodies such as run-of-the-river dams and excavated reservoirs through Object-Based Image Analysis, taking into account other image features such as shape and spatial relations.

Additionally, the method appears to be efficient in the present study because of the large number of available images that limit the uncertainty about the final decision to be taken after the data fusion stage. Nonetheless, in areas with permanent high cloud cover rates, the method may be limited. This is especially true when the Fmask

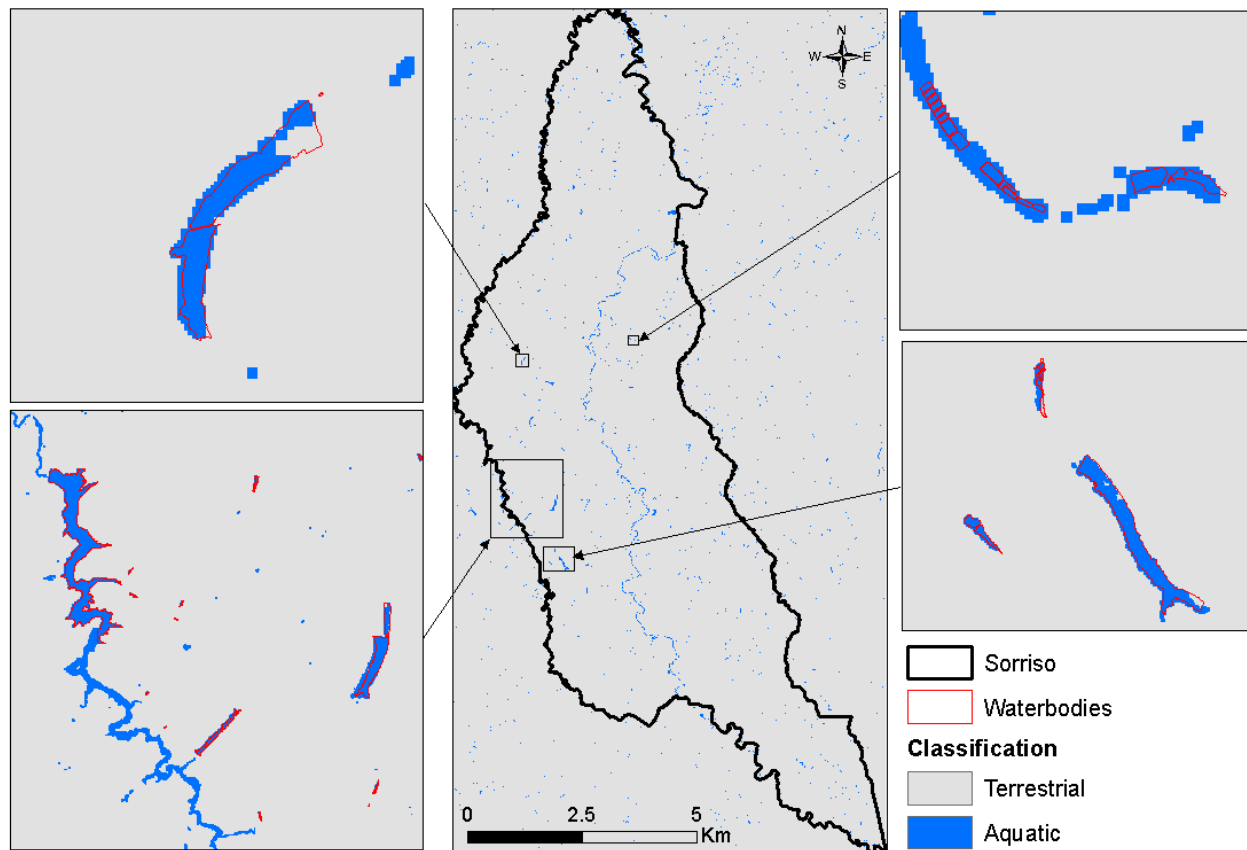


Figure 4. Classification of waterbodies in the municipality of Sorriso (MT) for year 2014.

algorithm does not correctly delimit all cloud shadows since shadow pixels may thus be assigned to semantic spectral categories corresponding to Aquatic land cover classes.

Nonetheless, the automation of the approach opens new interesting perspectives for geographic applications in the Southern Amazon. First, we intend to apply the method on pluri-annual time series in order to better understand when the emergence of artificial reservoirs started to increase. Second, we will apply the method at regional scale (i.e. Northern Mato Grosso) in order to test any spatial variability in the creation of water reservoirs between areas dedicated to large-scale export-oriented agriculture, small-scale agriculture or extensive cattle ranching. Finally, we will also apply the method at watershed scale (for instance, the Teles Pires watershed) to better assess the cumulative effect of these artificial water reservoirs on the hydrology, at local and regional scale.

6. CONCLUSION

The agricultural transition in the Southern Amazon based on the intensification and diversification of agricultural practices is considered as a major way to limit deforestation. However, it may also imply increased pressure on environment such as water resources. In the county of Sorriso, state of Mato Grosso, we implemented an automatic methodology to classify aquatic areas in order to illustrate our hypothesis. We mapped 19.5 km² of artificial reservoirs that emerged along the last decades for many purposes and whose environmental impacts remain understudied to date.

ACKNOWLEDGMENTS

The authors wish to thank the French National Agency for Research (ANR) which funded the DURAMAZ2 project (grant agreement ANR-11-BSH1-0003) and the European Union which funded the H2020-MSCA-RISE-2015 ODYSSEA project (Project Reference: 691053).

REFERENCES

- [1] Fearnside, P. M., “Soybean cultivation as a threat to the environment in Brazil,” *Environmental Conservation*, 23–38 (Mar. 2001).
- [2] Morton, D. C., DeFries, R. S., Shimabukuro, Y. E., Anderson, L. O., Arai, E., Espirito-Santo, F. d. B., Freitas, R., and Morissette, J., “Cropland expansion changes deforestation dynamics in the southern Brazilian Amazon,” *Proceedings of the National Academy of Sciences* **103**, 14637–14641 (Sept. 2006).
- [3] IBGE, “Instituto Brasileiro de Geografia e Estatística,” (2014).
- [4] INPE, “Metodologia para o Cálculo da Taxa Anual de Desmatamento na Amazônia Legal,” tech. rep. (2014).
- [5] Arvor, D., Meirelles, M., Dubreuil, V., Bgu, A., and Shimabukuro, Y. E., “Analyzing the agricultural transition in Mato Grosso, Brazil, using satellite-derived indices,” *Applied Geography* **32**, 702–713 (Mar. 2012).
- [6] Nepstad, D., McGrath, D., Stickler, C., Alencar, A., Azevedo, A., Swette, B., Bezerra, T., DiGiano, M., Shimada, J., Seroa da Motta, R., Armijo, E., Castello, L., Brando, P., Hansen, M. C., McGrath-Horn, M., Carvalho, O., and Hess, L., “Slowing Amazon deforestation through public policy and interventions in beef and soy supply chains,” *Science* **344**, 1118–1123 (June 2014).
- [7] Nepstad, D., Soares-Filho, B. S., Merry, F., Lima, A., Moutinho, P., Carter, J., Bowman, M., Cattaneo, A., Rodrigues, H., Schwartzman, S., McGrath, D. G., Stickler, C. M., Lubowski, R., Piris-Cabezas, P., Rivero, S., Alencar, A., Almeida, O., and Stella, O., “The End of Deforestation in the Brazilian Amazon,” *Science* **326**, 1350–1351 (Dec. 2009).
- [8] Arvor, D., Dubreuil, V., Ronchail, J., Simes, M., and Funatsu, B. M., “Spatial patterns of rainfall regimes related to levels of double cropping agriculture systems in Mato Grosso (Brazil): Spatial patterns of rainfall regimes in Mato Grosso,” *International Journal of Climatology* **34**, 2622–2633 (June 2014).
- [9] Funatsu, B. M., Dubreuil, V., Claud, C., Arvor, D., and Gan, M. A., “Convective activity in Mato Grosso state (Brazil) from microwave satellite observations: Comparisons between AMSU and TRMM data sets: CONVECTION IN MATO GROSSO FROM MICROWAVE,” *Journal of Geophysical Research: Atmospheres* **117**, n/a–n/a (Aug. 2012).
- [10] Arvor, D., Dubreuil, V., Simões, M., and Bgu, A., “Mapping and spatial analysis of the soybean agricultural frontier in Mato Grosso, Brazil, using remote sensing data,” *GeoJournal* **78**, 833–850 (Oct. 2013).
- [11] Arvor, D., Dubreuil, V., Mendez, P., Ferreira, C. M., and Meirelles, M., “Développement, crises et adaptation des territoires du soja au Mato Grosso: l’exemple de Sorriso,” *Confins* (June 2009).
- [12] Arvor, D., Jonathan, M., Meirelles, M. S. P., Dubreuil, V., and Durieux, L., “Classification of MODIS EVI time series for crop mapping in the state of Mato Grosso, Brazil,” *International Journal of Remote Sensing* **32**, 7847–7871 (Nov. 2011).
- [13] FAMATO and IMEA, “Diagnóstico da Piscicultura em Mato Grosso,” tech. rep., Federação da Agricultura e Pecuária do Estado do Mato Grosso and Instituto Mato-Grossense de Economia Agropecuária, Cuiabá-MT (2014).
- [14] Zhu, Z. and Woodcock, C. E., “Object-based cloud and cloud shadow detection in Landsat imagery,” *Remote Sensing of Environment* **118**, 83–94 (Mar. 2012).
- [15] Baraldi, A., Puzzolo, V., Blonda, P., Bruzzone, L., and Tarantino, C., “Automatic Spectral Rule-Based Preliminary Mapping of Calibrated Landsat TM and ETM+ Images,” *IEEE Transactions on Geoscience and Remote Sensing* **44**, 2563–2586 (Sept. 2006).
- [16] Irons, J. R., Dwyer, J. L., and Barsi, J. A., “The next Landsat satellite: The Landsat Data Continuity Mission,” *Remote Sensing of Environment* **122**, 11–21 (July 2012).

- [17] Di Gregorio, A., Food and Agriculture Organization of the United Nations, and United Nations Environment Programme, [*Land cover classification system: classification concepts and user manual: LCCS*], no. 8 in Environment and natural resources series, Food and Agriculture Organization of the United Nations, Rome, software version 2 ed. (2005).
- [18] Shafer, G., [*Mathematical Theory of Evidence*], Princeton University Press, Princeton, princeton ed. (1976).
- [19] Le Hégarat-Mascle, S., Seltz, R., Hubert-Moy, L., Corgne, S., and Stach, N., “Performance of change detection using remotely sensed data and evidential fusion : comparison of three cases of application,” *International Journal of Remote Sensing* **27**(15-16), 3515–3532 (2006).
- [20] Lu, Y., Trinder, J., and Kubik, K., “Automatic Building Detection Using the Dempster-Shafer Algorithm,” *Photogrammetric Engineering & Remote Sensing* **72**(4), 395–403 (2006).
- [21] Lefebvre, A., Sannier, C., and Corpetti, T., “Monitoring urban areas with sentinel-2a data: Application to the update of the copernicus high resolution layer imperviousness degree,” *Remote Sensing* **8**(7), 606 (2016).
- [22] Congalton, R. G., “A review of assessing the accuracy of classifications of remotely sensed data,” *Remote Sensing of Environment* **37**, 35–46 (July 1991).